

## Article

# Stone Endurance: A Comparative Analysis of Natural and Artificial Weathering on Stone Longevity

Carla Lisci <sup>1,2</sup> , Fabio Sitzia <sup>1,2</sup>, Vera Pires <sup>1,3</sup> , Marco Aniceto <sup>4</sup> and José Mirão <sup>1,2,\*</sup> 

- <sup>1</sup> HERCULES Laboratory and IN2PAST, Associate Laboratory for Research and Innovation in Heritage, Arts, Sustainability and Territory, Institute for Advanced Studies and Research, University of Évora, Largo Marquês de Marialva 8, 7000-809 Évora, Portugal; clisci@uevora.pt (C.L.); fsitzia@uevora.pt (F.S.); vlcp@uevora.pt (V.P.)
- <sup>2</sup> Geosciences Department, School of Sciences and Technology, University of Évora, Rua Romão Ramalho 59, 7000-671 Évora, Portugal
- <sup>3</sup> LEM Laboratório de Ensaios Mecânicos, da Universidade de Évora, R. Romão Ramalho 59, 7000-671 Évora, Portugal
- <sup>4</sup> SOLANCIS, Sociedade Exploradora de Pedreiras, S.A. Rua da Sindocal 22, Casal do Carvalho, Apartado 90, 2475-016 Benedita, Portugal; marco.aniceto@solancis.com
- \* Correspondence: jmirao@uevora.pt

**Abstract:** The long-term endurance of building stones must be assured since their longevity has repercussions for their economic and social value. Frequently, slabs for flooring and cladding are installed with polished finishing in outdoor environments for technical and ornamental purposes in cultural heritage sites and modern civil architecture. Compared to any other finishing, glossy surfaces are rather vulnerable to wear, particularly when they interact with slightly acidic rainwater. Several hydrophobic treatments are applied to prevent this damage by preventing contact between rain and stone; such treatments are efficient but sometimes non-durable. Stakeholders and conservation scientists need better methods to anticipate the future behaviour of this building material and hydrophobic solutions. Complying with this demand, a comparison is made between outdoor natural ageing and artificial weathering, reproduced by UVA radiation, moisture and spray accelerated weathering. Artificial weathering is applied to predict the behaviour of stones over time in the real environment. Data obtained through the measurement of gloss and colour parameters, the detection of micro-textures through SEM, and the calculation of micro-roughness using a digital rugosimeter demonstrate that weakly acidic rainwater is the main cause of superficial decay of stone finishing over just six months of outdoor exposure. This period corresponds to 7–14 days of artificial weathering. Furthermore, the loss of efficiency and durability of the hydrophobic coatings is detected by measuring the static contact angle. This highlights that even if a protective treatment was proficient, it could easily deteriorate in normal weathering conditions if applied on polished, low-porosity stone. Additionally, water vapour permeability indicates variations of regular vapour transmission through the stones due to ageing. The first solution to threats is the prevention of pathologies, including aesthetic ones. A careful choice of the most suitable lithotype finish and an environmental study represent an existing solution to the problem. It must be highlighted that aesthetic requirements should not be prioritised to detriment of the technical requirements of architectural quality, performance, durability, and safety.

**Keywords:** stone longevity; coating durability; building stones; heritage and architecture; stone transformation



**Citation:** Lisci, C.; Sitzia, F.; Pires, V.; Aniceto, M.; Mirão, J. Stone Endurance: A Comparative Analysis of Natural and Artificial Weathering on Stone Longevity. *Heritage* **2023**, *6*, 4593–4617. <https://doi.org/10.3390/heritage6060244>

Academic Editors: Mauro Francesco La Russa and Patricia Sanmartín

Received: 5 May 2023

Revised: 28 May 2023

Accepted: 1 June 2023

Published: 2 June 2023



**Copyright:** © 2023 by the authors. Licensee MDPI, Basel, Switzerland. This article is an open access article distributed under the terms and conditions of the Creative Commons Attribution (CC BY) license (<https://creativecommons.org/licenses/by/4.0/>).

## 1. Introduction

The long-term durability of building stones and the efficiency of protective coatings have economic and social repercussions and must therefore be assured. Stakeholders need to know how long building stones are resistant to weathering. Thus, a comparison between

outdoor (or natural) ageing and artificial weathering is necessary to better predict the behaviour of building elements [1].

Several standards for natural stones were created to artificially simulate natural ageing, namely aggravation practice tests used to obtain results quickly [2], including: (i) freeze-thaw [3] and thermal shock resistance tests [4]; (ii) salt crystallisation tests via saturation in concentrated saline solutions [5] and concentrated salt fog in the atmosphere [6]; (iii) SO<sub>2</sub> action tests in the presence of humidity [7]; and (iv) high UV exposure tests for assessing the durability of protective coatings [8].

The correlation between natural and artificial ageing is not universal, because the decay depends on the lithotypes and their heterogeneity, besides a wide variety of climatic-microclimatic conditions. In the laboratory, an exact simulation of outdoor weathering is complex due to the difficulties associated with the combined reproducibility of climatic parameters such as temperature, thermal variations, humidity, moisture, rain, UV radiation, wind action, wind-driven rain, salt presence, biological colonisation, and CO<sub>2</sub>, SO<sub>x</sub>, and NO<sub>x</sub> compounds.

Usually, just a few parameters can be controlled in a climatic chamber, most commonly temperature, humidity, moisture, spray (for simulating rain), and UV radiation. Real values acquired by meteorological stations must be used to programme a climatic chamber [9]. Nowadays, climatic chamber design has improved, and researchers are developing protocols and diverse setups to increase the realism of climate reproductions in the laboratory.

A standard dedicated to artificial weathering in climatic chambers for natural stones treated with hydrophobic treatments or other coatings does not exist yet. Protocols are still in progress and their validation and harmonisation are challenging for the scientific community, companies, and standardisation bodies.

Only some standards [10–12] and EOTA technical reports [13] are dedicated to studying the durability of coatings composed of organic or inorganic materials (i.e., ink, paints, varnishing, roofing, bitumen membrane etc.) under artificial light exposure (from xenon arc light sources or fluorescent UV light source). Some of these cited standards include heating/spray/moisture cycles associated with the effects of UV light. The EN 17036 standard is available for the durability evaluation of coatings for porous inorganic materials used in cultural heritage sites [14]. All of these standards allow a preliminary selection of the most suitable products to use in a specific case of intervention.

The long-term effects of weather in a Dfb climate (warm-summer humid continental climate) were monitored over 545 days to assess changes in the properties of poly(alkyl siloxane), poly(alkyl siloxane) + nano-ZnO, and hydrophobics on Mšené sandstone, which is widely used in several monuments listed by UNESCO [15]. The study occurred in Ostrava (Czech Republic), where high air pollution enabled evaluation of the durability of the formulations in severe conditions. Coated samples performed well, with  $\Delta E\% < 3.7\%$  ( $\Delta E\%$  is the colour difference expressed in %). The change in contact angle decreased from 3° to 15°. The presence of ZnO prevented algae growth, while in the other samples, biological colonisation was noticeable. Future goals of this study include the comparison of natural ageing with a simulated Dfb climate in a climatic chamber.

The influence of 30 years of outdoor weathering on the durability of hydrophobic agents (TEOS, silicone resins) applied on Obernkirchener Sandstones was studied [16]. Sandstones were analysed after 2, 24, and 30 years of natural weathering in residential, industrial, urban, and business environments with different anthropic impacts. This study also considers the mean temperature, relative humidity, amount of precipitation, and air quality. Colourimetry showed an elevated  $\Delta E > 5\%$ , higher than the value denoting noticeable difference [17], because of the formation of black crusts and biogenic growth. Water absorption and capillary absorption decreased and hydrophobic capacity increased according to the coating's formulation and penetration depth, even where biological colonisation allowed water retention on sample surfaces.

Few parallel studies comparing the two types of weathering have been performed by researchers.

Ten years of natural ageing in Turin (Italy) were compared with artificial ageing via thermal and moisture cycles (bowing test according to EN 16306) using marbles from Carrara [18]. Authors found that, in some marbles, porosity and bowing were more severe after ten years of natural ageing compared with the small changes observed after performing the artificial bowing standard test. As a result, the data led to a misunderstanding of the quality of the stones. Water absorption results were not consistently interpreted. Mechanical properties had the same variation after 30, 60, and 90 thermal cycles according to the accelerated bowing test method.

Other authors tested the durability of an acrylic coating applied on dolomite by correlating the results of an accelerated test (4000 h of 700 W/m<sup>2</sup> Xenon irradiation and light sources with wavelengths > 295 nm at 45 °C) with 60 months of real exposure in Florence (Italy) [19]. Infrared-spectroscopy and size-exclusion chromatography showed that the molecular weight distribution of the product changed after 500 h of artificial ageing, corresponding to 30 months of natural ageing. The protection efficacy after 30 months of outdoor exposure corresponds to that observed after 2500–3000 h of Xenon irradiation. Different correlations have also been found for other coating formulations.

The durability of a nanostructured sunlight-curable organic and inorganic hybrid protective coating for porous stones was assessed on Lecce Stone over 730 days of exposure and artificial weathering in a QUV chamber (UV chamber provided by Q-lab corporation) [20]. The QUV test time consisted of 4 cycles of 100 h of UVA exposure (340 nm) using a fluorescent lamp with an irradiance of 0.71 W/m<sup>2</sup> at 60 °C, followed by condensation at 50 °C for 4 h. An empirical correlation between the two weathering types has been found by measuring the contact angle and the  $\Delta E\%$ . The contact angle was >130° after 20 days of exposure in artificial weathering, while in an outdoor environment, this value was reached after 730 exposure days. The  $\Delta E\%$  was equal to 4.5 after both 20 cycles and 730 days as well. Experimental tests suggested that the coating could be durable for up to twelve years in natural weathering conditions.

A new climatic chamber setup for the estimation of stone decay was proposed [21,22]. In the current study, the authors continue the investigation comparing the changes obtained with accelerated weathering. QUV-spray accelerated weathering over fourteen days was compared with the data achieved by exposing stones to six months of outdoor exposure in Evora (Portugal). The QUV-spray chamber is a piece of equipment provided by the Q-lab corporation that reproduces UV radiation and the spray of water. Regarding Portuguese building stones, the authors could not find any works dedicated to a comparative study between natural and artificial weathering. This study can open avenues for future investigation of Portuguese stone durability. Climatic parameters such as temperature, humidity, rainfall, and solar radiation were collected, and the physical characterisations of rainwater and QUV-spray water were determined.

Natural stone finishing influences the alteration forms and decay patterns of stone because it regulates water transport and interactions with the surface and substrate [23]. In rougher surfaces, deeper water retention leads to physical/mechanical decay, while polished finishings are more sensitive to aesthetic damage [24]. In contrast, rougher surfaces allow for better penetration of specific treatments, while polished finishing inhibits penetration. Low product penetration forms a superficial film that can easily deteriorate. Frequently, slabs for flooring and cladding are installed with polished finishing in outdoor environments for technical and ornamental purposes in cultural heritage sites and modern civil architecture. This study focuses on the durability of polished finishing on natural stone and the long-term efficiency of protected polished surfaces with hydrophobic coatings. The latter are widely used in slabs for flooring and cladding in outdoor environments. A polished surface is more suitable for building understanding of the chemical processes involved in weathering and for monitoring superficial modifications to stone (gloss, colour, texture). Additionally, polished finishing is suitable for evaluating the durability of hy-

drophobic coatings because it is easier to measure variations in static contact angles on a regular surface.

## 2. Materials and Methods

Natural stones from Portugal have been selected to lead this study because of their use in ancient, contemporary, and civil architecture, making them representative of typical vernacular architecture [25].

Selected lithotypes are: Lioz A (limestone), Lioz B (limestone), Lioz C (limestone), Alpinina (limestone), black and white marble (labelled BW marble), Rosa marble, and blue limestone (Figure 1).



**Figure 1.** Ancient and contemporary buildings built with Portuguese stones. Lioz limestones were used for constructing the (a) Belem Tower and (b) Palace of Parliament in Lisbon (Portugal). Rosa and BW marble were used in ancient architecture, as well as in (c) Estremoz Castle (Portugal) and (d) residential buildings in Lisbon; (e) Alpinina is used in civil modern architecture; (f) is an example of Azul limestone used as cladding with weathered polished finishing.

The selection of suitable materials for architectural projects is crucial in achieving both aesthetic appeal and functional excellence. In historic and recent times, Portuguese stones have gained significant recognition, owing to their demand for cladding applications (Figure 1).

Lioz limestone samples range from compact–very compact, and are coarse, bioclastic, pure limestones. Their commercial nomenclature depends on their colour, on the quantity of fossils, and on the presence of stylolithic joints with variable openings and frequencies, depending on their *facies* (Figure 2a,c,e).

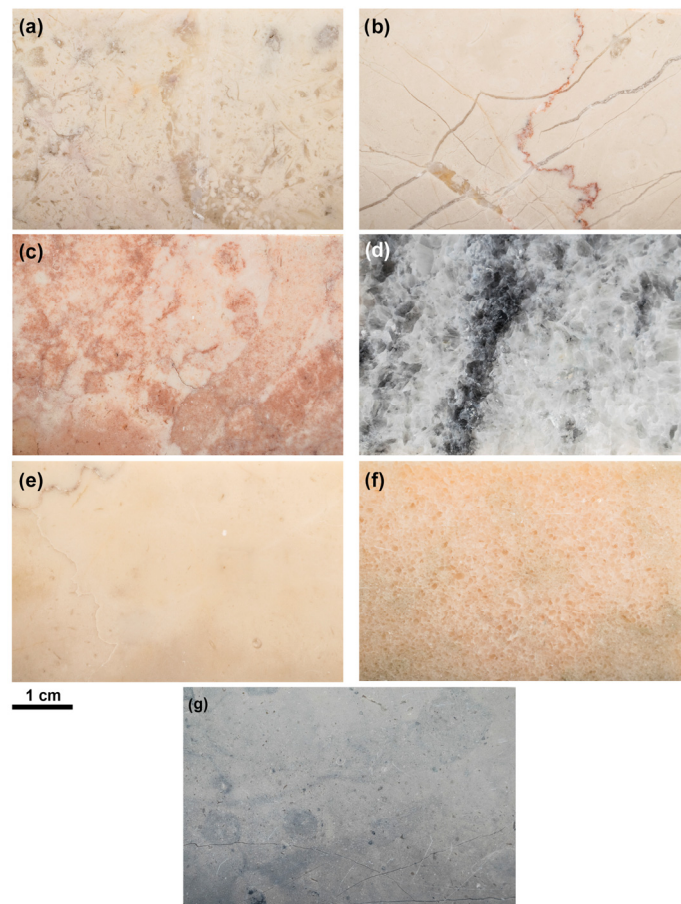


**Figure 2.** Macroscopic appearance of the lithotypes selected for this study. (a) Lioz A, (b) Alpinina, (c) Lioz B, (d) black and white marble, (e) Lioz C, (f) Rosa marble, (g) blue limestone.

Alpinina is a fine-grained limestone with a compact, beige colour. It contains closed stylolites, iron-rich veins, and bioclasts. This limestone has undergone intense tectonic activity and recrystallisation (Figure 2b).

Black and white marble (labelled BW in this text) is a white marble with large black veins. It is characterised by large calcite crystals with a granoblastic interlobate texture (Figure 2d).

Rosa is a pink marble with a medium-fine grain size. It shows grey veins, caused by the presence of oxides (Figure 2f).

Blue limestone is a gray blue calciclastic and bioclastic limestone. It is compact and characterised by the presence of abundant organic matter and other impurities. (Figure 2g).

Optical microscope (OM) observations were obtained using a Hirox HRX-01 digital microscope on 30  $\mu\text{m}$ -thick sections.

Colour data were collected before, during, and after ageing tests with a portable Data-Color CheckPlus II spectrophotometer. Colour distance,  $\Delta E_{ab}$ , was calculated according to the CIE76 formula [26] following Normative EN 15886 [27]:

$$\Delta E_{ab} = ((L_{\text{Post}} - L_{\text{Pre}})^2 + (a_{\text{Post}} - a_{\text{Pre}})^2 + (b_{\text{Post}} - b_{\text{Pre}})^2)^{0.5} \quad (1)$$

where  $L^*$  represents the brightness or intensity of the colour, and ranges from 0 to 100 (a value of 0 corresponds to black, and 100 to white);  $a^*$  represents the colour along the red-green axis (positive values are in the red region, while negative values in the green region); and  $b^*$  represents the colour along the yellow-blue axis (positive values represent the yellow region, while negative values represent the blue region).

The gloss of the stones was monitored using a Gloss Checker IG330 with an LED light source in the wavelength of 80 nm.

SEM analyses were performed with a HITACHI S3700N scanning electron microscope. This technique was appropriate for studying the micro-textures and modifications in roughness at the stone–water–air interface. Numerical parameters of roughness ( $R_a$ ,  $R_q$ , and  $R_z$ ) were obtained using a MITUTOYO SURFTEST SJ-210 (calibration standard by ISO1997). The measurements have been taken by selecting an exploration length of 4.80 mm and a sensor speed of 0.5 mm/s. The standard roughness,  $R_a$ , is defined as the arithmetic mean value of the deviations (taken as an absolute value) of the real profile of the surface with respect to the mean line.  $R_q$  is defined as the square mean of the deviations of the profile points from the mean line. It enables simple statistical management and allows for stable results because it is not significantly affected by scratches and contamination.  $R_z$  is defined as the distance between two lines parallel to the mean line passing, on average, between the five highest peaks and the five lowest valleys within the limits of the base length. Roughness was calculated before and after natural and artificial weathering.

The water vapour permeability test was carried out following the European CEN 15803 standard [28]. Specimens were previously dried in the oven for 24 h at  $60 \pm 5$  °C until a constant mass was reached. Samples were then placed in a dryer for 24 h prior to the permeability measurement. Each dried specimen was weighed to obtain the dry mass ( $m_d$ ). To create a 100% moisture saturated environment, cotton wool was placed in a permeability cup with 1 cm of distilled water. Each set (cup + water + specimen) was weighted ( $m_i$ ) and then placed inside an ARALAB FITOCLIMA 300 EDTU climate chamber. The chamber was programmed to 20 °C and 40% of relative humidity as required by the standard. Sets were weighed continuously every 24 h after the beginning of the test. The end of the test was reached when the sets achieved a mass difference equal to 0.1%. The water vapour flux ( $G_w$ ) was estimated from the average of the differences between masses per time unit (in g/h), using at least three values obtained in steady-state flow. Water vapour permeability ( $W_{VP}$ ) is given in  $\text{kg}\cdot\text{m}^{-1}\cdot\text{s}^{-1}\cdot\text{Pa}^{-1}$  through Equation (2), as follows:

$$W_{VP} = (G_w \times h) / (A_s \times \Delta P \times 36 \times 10^5) \quad (2)$$

where  $G_w$  is water vapour flux (g/h),  $h$  is the specimen thickness (m),  $A_s$  is the tested area ( $\text{m}^2$ ), and  $\Delta P$  is the pressure difference between water vapour inside and outside the cup (Pa). The reduction in the vapour permeability (RVP) was quantified as:

$$\text{RVP}\% = ((W_{VP\text{post}} - W_{VP\text{pre}}) / P_{\text{Pre}})100 \quad (3)$$

Water vapour permeability was measured before and after natural and artificial ageing.

The weight of the samples/cups was measured using a KERN & Sohn ABS 220-4 scale after 164 h of drying until the constant mass was reached.

In the QUV-spray chamber, the samples were subjected to weathering cycles according to the ASTM G154-C.7 standard [12]. This standard consists of 8 h of UVA radiation with a wavelength of 340 nm at 60 °C ( $1.55 \text{ W}/\text{m}^2$  irradiance), with 15 min on spray mode (7l/m of MilliQ-water) and 3:45 h of condensation at 50 °C. One cycle lasts 12 h. The test took 14 days. The gloss, colour, and weight of the samples were measured before ageing and after 3, 7, and 14 days of ageing. Samples placed in the climatic chamber had dimensions of  $12 \times 6 \times 1$  cm.

The static contact angle was measured according to EN 15802 [29] using a Ramé-hart 210-U4 goniometer/tensiometer with a fiber optic illuminator and a SuperSpeed digital camera operating at 520 frames/second. DROPimage Pro software was used to process the images. It allowed the evaluation of the wettability degree of the stones after the application of hydrophobic treatments.

Total dissolved solids (TDS), temperature, pH, and conductivity of water was measured with a PANCELLENT TDS&Ec meter and HANNA HI99171. Total hardness, total alkalinity, and carbonate were measured with an eXact<sup>®</sup> Micro 7+ photometer.

The mineralogical composition of the desert dust storm that occurred during the natural exposure was characterised using  $\mu$ -XRD with a Bruker D8 Discover diffractometer (Bruker Company, AXS Karlsruhe, Germany), with a  $\text{CuK}\alpha$  radiation tube running at 40 kV and 40 mA. The XRD peaks were measured between  $2^\circ$  and  $75^\circ 2\theta$ , with 1s counting time per point. The Powder Diffraction Database (PDF-ICDD, International Centre for Diffraction Data), using the Bruker EVA software, allowed the identification of the crystalline phase.

### 3. Climatic Data, Physical Analyses of Rainwater and QUV-Spray Water

Samples were exposed in the real environment and subjected to natural/outdoor weathering in Évora (Portugal). Daily climatic parameters were collected from the Institute of Earth Sciences (University of Evora database) from November 2021 to April 2022 and included the minimum, maximum, and average temperatures ( $T\text{ }^\circ\text{C min}$ ,  $T\text{ }^\circ\text{C max}$ ,  $T\text{ }^\circ\text{C av.}$ ) and the relative humidity (rH %), rainfall levels (mm), and solar radiation ( $\text{W}/\text{m}^2$ ). Climatic data are the key for understanding the contribution of each climatic factor in the decay of building stones.

December 2021 and March 2022 were the rainiest months, characterised by 96.9 mm and 134.7 mm of rainfall accumulation, respectively (see Annex 1). Samples exposed to the natural environment had dimensions of  $12 \times 6 \times 1$  cm, the same of those placed in the QUV-spray climatic chamber.

Physical-chemical analyses of the rainwater and QUV-spray water also significantly contribute to building understanding of the stone damage. The values of total dissolved solids (TDS, ppm), electric conductivity (EC,  $\mu\text{S}/\text{cm}$ ), and water pH are presented in Table 1.

**Table 1.** Physical-chemical analyses of rainwater and QUV-spray water collected for the study.

Date of Sampling	TDS (ppm)	EC ( $\mu\text{S}/\text{cm}$ )	T ( $^\circ\text{C}$ )	pH
27 December 2021 after 1 week of rain	57	98	17	6.24
13th February 1 day of rain; wind S.W. direction	138	276	10	8.07
26th February 1 day of rain	30	53	10	7.41
13th March 1 week of rain	11	29	9.5	5.93
24th March 5 days of rain	5	10	11	6.5
5th Apri 11 day of rain	15	30	10	6.64
12th Apri 12 days of rain; wind S direction	32	64	14	6.73
24th Apri 14 days of rain	4	8	10	6.47
QUV-spray chamber water	<1	<0.1	20	6.45

According to the [www.ventusky.com](http://www.ventusky.com) (accessed on 16 March 2022) database, the air quality index (AQI) of Évora is good (see Annex 2). According to the database, values of  $\text{O}_3$ ,  $\text{NO}_2$ ,  $\text{SO}_2$ , CO,  $\text{PM}_{2.5}$ , and  $\text{PM}_{10}$  posed little or no risk for human health, except on the 17th of March, when a desert dust plume arrived in the city. In that case, the maximum dust load registered was  $305\ \mu\text{g}/\text{m}$ . A semi-quantitative analysis of the Saharan dust performed through X-ray diffraction identified quartz (50%), microcline (17.1%), gypsum (15.4%), illite (9.4%), and albite (8.1%). The presence of these minerals in the atmosphere was recognised by its buffer effect and its influence on the pH of rain [30], which led to pH values higher than 5.6 [31]. In this study, the pH during a rain event during a desert dust storm was 8.07.

#### 4. Hydrophobic Solutions and Application Method

Hydrophobic coatings used are as follows: (i) aminopropyltriethoxysilane ( $C_9H_{23}NO_3Si$ ), labelled coating 1; (ii) aminopropyltriethoxysilane in 1:2 dilution, labelled coating 2; and (iii) tripotassium propylsilanetriolate ( $C_3H_7K_3O_3Si$ ), labelled coating 3. Products were applied by rolls, avoiding any excess for a controlled application, as suggested by producers.

Physical properties such as specific weight, dry residue, colour, the type of solvent, and the pH of the products are specified in Table 2.

**Table 2.** Physical properties of the hydrophobic coatings used for protecting the stone surfaces. N.A.: not available.

	Aminopropyltriethoxysilane	Tripotassium Propylsilanetriolate
Specific weight (kg/L)	$0.82 \pm 0.05$	N.A.
Dry residue (%)	$7 \pm 0.02$	$48 \pm 3$
Colour	colourless	colourless
Solvent	xilene	water
pH	N.A.	>13

#### 5. Results and Discussion

##### 5.1. Sample Characterisation by Optical Observations

Lioz A (Figure 3a) is characterised by a depositional grain-supported texture. The stone is composed of about 50% sparitic cement, while about 48% of the thin section consists of bioclasts (corals, bivalves, and other fossils). The estimated porosity is around 2%. According to the Folk classification [32], it is classified as biosparite.

In the case of Lioz B (Figure 3b), the sparitic cement content is  $\approx 85\%$  of the thin section, and micro-stylolites with a maximum opening of 10  $\mu m$  are visible. Fragments of crystals (calcite and opaque minerals) were detected with a content of 3%. Additionally, bioclasts of echinoderms, gastropods, and bivalves were detectable ( $\approx 10\%$ ). The primary porosity is between 1 and 2%. According to the Folk classification, the stone is classified as biosparite.

Lioz C (Figure 3c) has a mud-supported depositional texture, with a micritic matrix accounting for 94% of its makeup. Recrystallised sparitic calcite veins are present in a concentration of 5%. These veins range from 500  $\mu m$  to 1 mm, with thick openings and irregular spacing. Rare opaque minerals attributable to iron oxides were also detected. Some bioclasts of coralline algae, bryozoans, and foraminifera were identified in the thin section (1%). According to the Folk classification, Lioz C is a biomicrite.

Alpinina (Figure 3d) is a slightly metamorphosed limestone. It is characterised by a micritic mud-supported matrix that accounts for 80% of its makeup. The remaining 20% of the thin section shows subparallel recrystallised sparitic veins with variable spacing and openings in the range of 0.1 mm–5 mm. Bioclasts of foraminifera, gastropods, bivalves, echinoids, and ostracods are recognisable. Diffuse peloids smaller than 0.5 mm are also observed. According to Folk classification, Alpinina is an intermediate form of pel-biomicrite-sparite.

BW (Figure 3e) is a calcitic marble with a homeoblastic, isotropic, and granoblastic interlobate texture. The maximum grain size (MGS) of calcite crystals is 8 mm, with an average size of 5 mm. The grain boundary shape (GBS) is mainly curved, toothed, and partly straight. Sub-millimetric inclusions of well-rounded quartz, pyroxene, iron oxides, and opaque phases are detected ( $\approx 2\%$ ).

Rosa (Figure 3f) has a homeoblastic, semi-polygonal granoblastic-oriented and isotropic texture. The MGS is 2 mm and the average grain size is 1.2 mm. The GBS is mainly straight and secondarily curved. 98% of the rock crystals are calcitic, with 2% sub-millimetric inclusions of opaque minerals (10  $\mu m$ ) and quartz (200  $\mu m$ ).

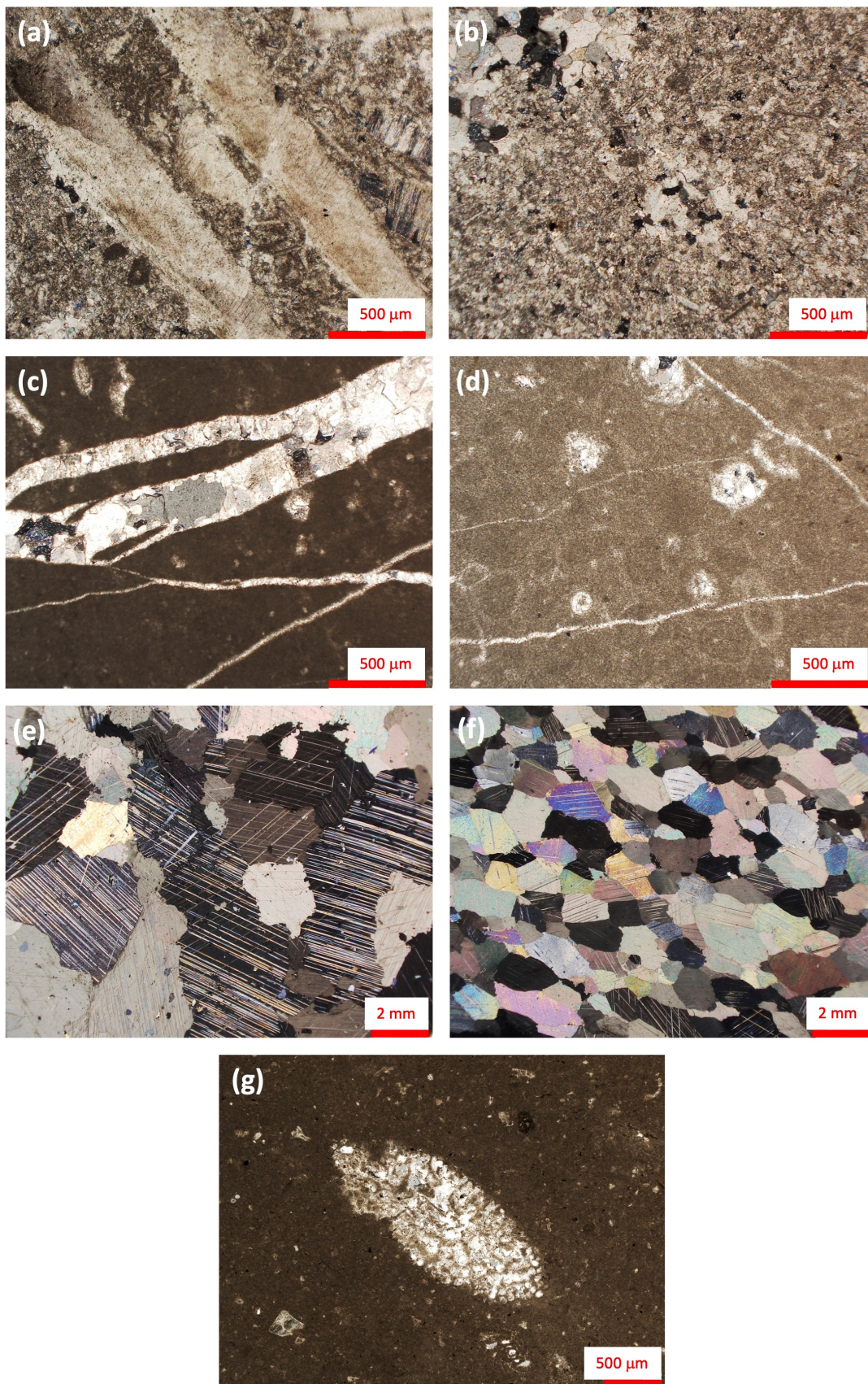


**Figure 3.** Characterisation through optical observations: (a) Lioz A (biosparite), (b) Lioz B (biosparite), (c) Lioz C (biomicrite), (d) Alpinina (pel-biomicrite-sparite), (e) BW marble, (f) Rosa marble, (g) blue limestone (biomicrite).

Blue limestone (Figure 3g) is characterised by a micritic matrix (>90% vol.) with a clay mineral content of <2%. Allochem crystals of quartz in a range from 0.4 to 1.8% vol. have been recognised. The organic matter is up to 6% vol. The bioclastic component is also relevant. According to Folk, the stone is classified as biomicrite.

## 5.2. Aesthetic Modifications

### 5.2.1. Gloss Monitoring

Gloss measurements with 60° of reflected light (Figure 4) showed a decrease in gloss after 1 week of rain, passing from 56 to 31 in Lioz A, from 15 to 4 in Lioz B, from 14 to 6 in Lioz C, and from 72 to 16 in Alpinina. In marbles, gloss decreased from 87 to 62 in BW and from 70 to 35 in Rosa. Blue limestone almost completely lost its gloss (3 gloss units on 27 December 2021, 1 gloss unit on 3 January 2022).

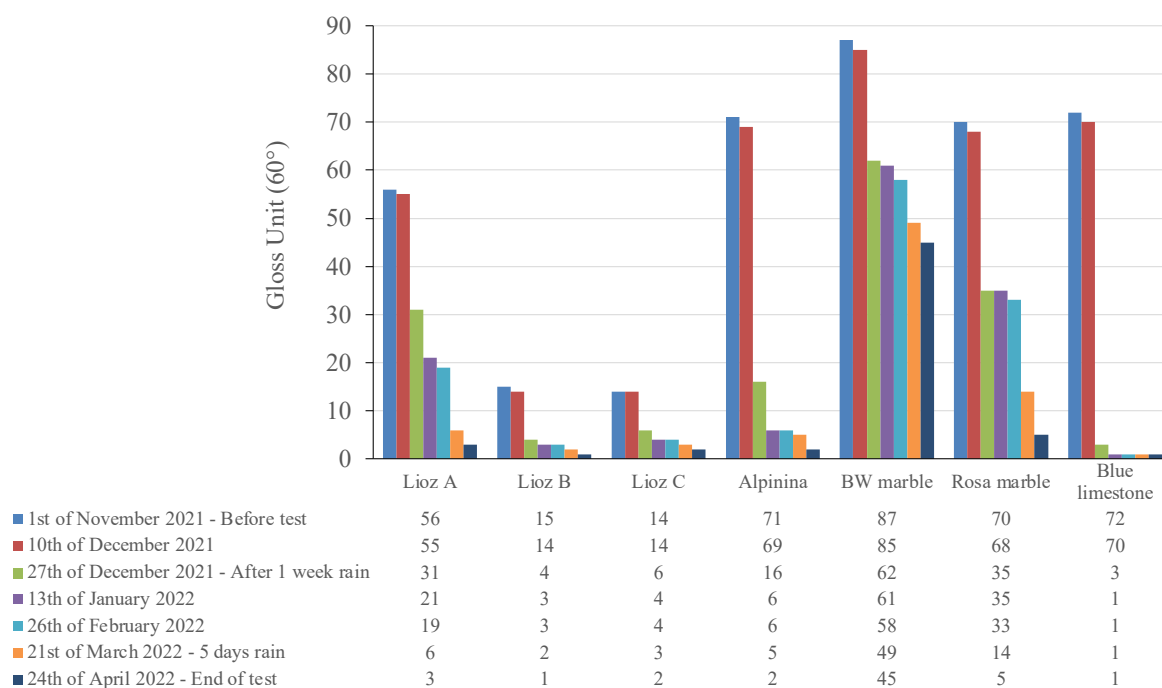


**Figure 4.** Gloss unit variation (60° reflected light) for each stone before and during the outdoor ageing, correlated with the date of collection of the rainwater. Histograms show the gloss reduction mainly after rain events (27 December 2021 and 21 March 2022).

Blue limestone normally suffers from rapid decay due to the abundant presence of pyrite that easily oxidises in the presence of water (liquid and moisture), oxygen, organic matter, and clays. These impurities act as an accelerating factor in aesthetic, physical, and mechanical damage, even in the short term [33,34], causing micropore modification, which affects the durability of the stones [35,36].

By matching the gloss with the physico-chemical analyses of the rainwater, it is clear that water with a pH of 6.24 is responsible for the dissolution of the matrix, having a corrosive effect on the carbonate surface and causing important modifications of the superficial finishing. The relatively low concentration of total dissolved solids (TDS = 57 ppm at the moment of sampling) permits water to absorb more gaseous CO<sub>2</sub>, leading to the formation of carbonic acid that turns the water slightly acidic.

The absence of gloss reduction after the 13th and 26th of February cannot be ignored. Despite the higher pH levels (8.4 and 7.41) and TDS values of up to 138 ppm in the rainwater collected on these days, it is unlikely that they would have the same dissolving effect as hypothesised on 27 December after a week of continuous rain. This is further supported by the fact that the wind blew from S.W., originating from Northern Africa, which could explain the elevated TDS levels. In February, the main climatic parameters

that could potentially cause a change in gloss are relative humidity and, secondarily, UV radiation. However, it appears that the superficial finishing was not significantly altered by this factor, except in the cases of Lioz A, where the gloss decreased from 31 to 21 in just 17 days, and Alpinina, where it dropped from 16 to 6. The data collected after the 13th and 26th of February challenges the earlier hypothesis that rainwater pH and TDS are the primary causes of gloss reduction. The influence of relative humidity cannot be overlooked, and further investigation is warranted to fully understand the complex dynamics of gloss changes for different lithologies. The presence of sparite in Lioz A and Alpinina limestones could suggest a higher susceptibility of these lithotypes, as also detected by other researchers [36,37]. Furthermore, Lioz A had another gloss decrease after 5 days of rain in March, illustrating the general tendency of the stone to equilibrate with the weather conditions due to the abundant presence of sparite.

Regarding the marbles, the gloss of BW decreased after 1 week of rain registered in December (from 67 to 62 gloss units). Gloss of Rosa marble reduced from 70 to 35. This was an unexpected result, because gloss is normally conferred by the natural reflectance of the calcite crystals in marble. This superficial alteration confirms that the physical parameters of the rainwater also opacified the polished finishing of marbles. After that, another important variation occurred after 5 days of rain in March, where a pH of 6.5 and a TDS of 5 ppm drove another dissolution period of the stone.

Interpreting the gloss variation monitored after the QUV-spray ageing (Figure 5), a radical decrease in the gloss unit occurred only after three days of ageing in most samples, except in BW and Rosa marbles. Compared with the results obtained after natural ageing, it can be stated that, in this case, three days of QUV-spray chamber ageing correspond to five months of natural ageing. In blue limestone, the correlation is just two months. Considering that, from 1 November to 27 December, just a few mm of rain fell and a minimal reduction in gloss emerged, three days of natural ageing correspond to four months, highlighting that the most important variation took place after 1 week rain in December.

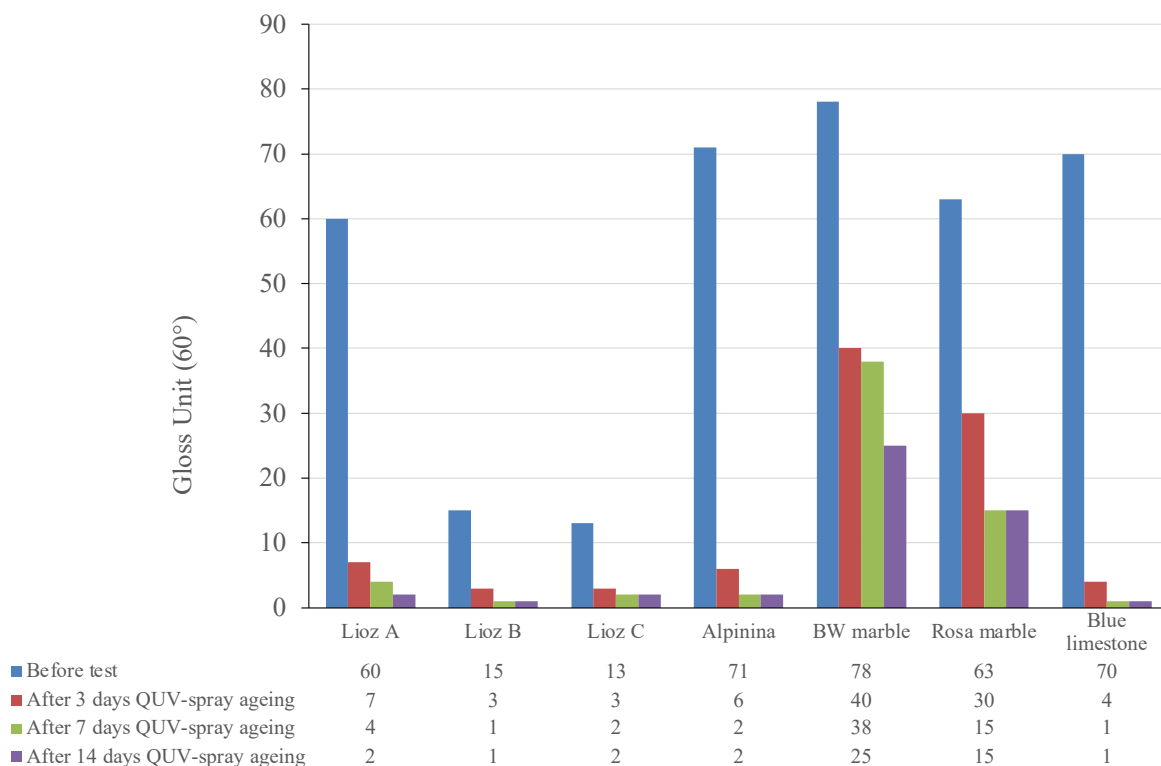


**Figure 5.** Gloss variation (60° reflected light) for each stone before the QUV-spray ageing and after 3, 7, and 14 days.

The gloss of BW marble was stable at 45 until 24 April, after 6 months of natural ageing, whereas it decreased to 40 after 3 days of QUV-spray ageing, stabilizing at 25 after 14 days of ageing. This means that BW, being a marble with coarse texture, takes more than several months of winter to lose its polished finishing.

The same considerations can be made regarding the blue limestone treated with hydrophobics. After one week of rain, the gloss of the samples was drastically reduced (Figure 6a). This was an unexpected result. Concerning coating 1, it presented 8 gloss units instead of the 3 observed during the natural ageing of the untreated blue limestone on the same date and maintained a value of 4 until 26 February 2022. The stone completely lost the gloss after five days of rain ending on 21 March 2022, while the uncoated blue limestone lost the gloss on 13 January after twenty-five days of rain since the beginning of the experiment. Additionally, blue limestone treated with coatings 2 and 3 lost its gloss on 13th of January.

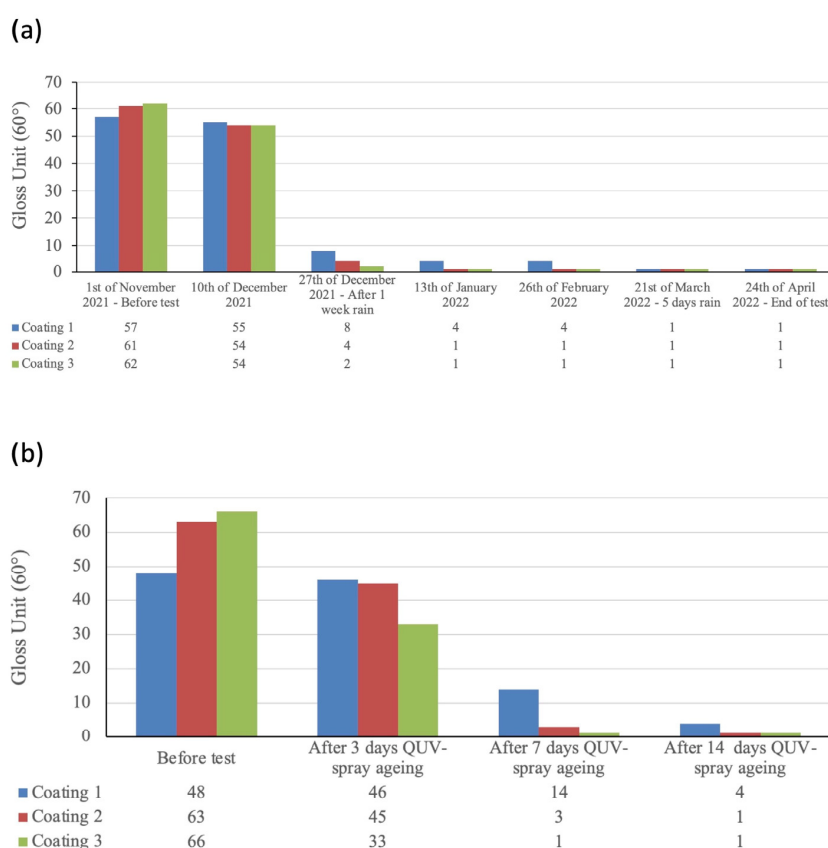


**Figure 6.** (a) Gloss variation in blue limestone treated with protective coatings before and during the outdoor ageing. Additionally, in this case the graph points out the gloss reduction mainly after rain events (27 December 2021 and 21 March 2022). (b) Gloss unit variation ( $60^\circ$  reflected light) for blue limestone treated with protective coatings. Coating 1 (aminopropyltriethoxysilane), coating 2 (aminopropyltriethoxysilane in 1:2 dilution), coating 3 (tripotassium propylsilanetriolate).

Different results were acquired for coated samples subjected to QUV-spray ageing (Figure 6b). They preserved a certain level of gloss after three days of artificial ageing, as observed from coating 1, which retained some gloss after seven days and a residual value after 14 days. The gloss differences are very relevant when compared to the uncoated blue limestone after one week of rain in December 2021, and also when compared to the blue limestone that was artificially aged for three days. It can be stated that all hydrophobic materials are more efficient in the climatic chamber than in outdoor exposure, as was observed by other authors [18]. During natural ageing, the rainfall accumulation registered in December 2021 was 96.91 mm, concentrated mostly during one week (from the 20th

to the 27th), and had a pH of 6.25 and a TDS of 11. In March 2022, from the 20th to the 24th 134.723 mm rainfall accumulated with a pH of 6.5 and a TDS of 11. Additionally, the rainwater collected after four rainy days ending on 13 March 2022 had a pH of 5.93 (Table 1).

### 5.2.2. Colour Distance

In Figures 7 and 8, colour distances, expressed as  $\Delta E\%$  of the stones after different durations of natural and artificial ageing, are shown.

A general whitening effect was observed due to the rising luminance (L parameter) of the samples after natural ageing and after QUV-spray ageing of the polished surface. Some key observations about the factors responsible of that behaviour are discussed.

The stones are composed primarily of calcium carbonate ( $\text{CaCO}_3$ ). Their mineralogical compositions hold impurities such as clay, quartz, and iron oxide, which affect their colour and weathering characteristics. Furthermore, the presence of micrite and sparite in varying percentages can result in different behaviour during several climatic/ageing conditions. Marbles are metamorphic rocks formed from limestone that has undergone recrystallisation due to high temperature and pressure. This often results in a mineralogical phase transition, and they have a different fabric compared to limestone. These attributes impact the varying colour distance between limestone and marble, which may not be reliably correlated with the time of natural weathering and artificial ageing.

Natural weathering of limestone and marble is a complex process that is influenced by various environmental factors such as temperature, humidity/moisture, rainfall, wind, and exposure/orientation to sunlight. Therefore, the rate and extent of weathering may not be faithfully reflected by the colour distance calculated in a specific moment. The trend of colour distance measured is, for this reason, quite irregular, and it was not possible to find any reliable correlation between the duration of weathering and the widening of chromatic alteration.

The effect of the QUV-spray chamber had a more aggressive effect on the colour distance increment after up to fourteen days of ageing, except for Lioz A and Lioz C, which had different degrees of gloss ( $60^\circ$  and  $13^\circ$ , respectively). A regular increase in  $\Delta E\%$  can be noticed, probably due to the limited controlled and fixed parameters of the ASTM G154-cycle7. Photochemical reactions occur in light-sensitive minerals such as calcite that can undergo discolouration. Stones were exposed to  $1.55 \text{ W/m}^2$  UVA radiation, moisture, and high temperatures, resulting in a change in their colour. Stone surfaces suffered physical damage as well when moisture at high temperatures interacted with their matrices, resulting in thermal shock, as declared by the producer. This can result in a modification of the macroscopic appearance and colour of the minerals, also affecting the marbles, which are supposed to be more resilient.

The surface finish and texture of limestone and marble also impact their colour and weathering behaviour. Polished limestone or marble will have a different surface texture compared to unpolished or rougher surfaces (sawed, flame-treated, etc.), resulting in differences in colour perception. This point will be detailed in the next paragraph.

In general,  $\Delta E\%$  does not permit a temporal correlation between natural and artificial ageing in each case due to the wavering trend emerging during the outdoor exposure, as pointed out by [21,38]. Conversely, QUV-spray showed a correlation between temperature, humidity, UVA radiation, and spray.

Additionally, in the blue limestone protected with hydrophobics (Figure 8),  $\Delta E\%$  does not permit a reliable temporal correlation between natural and artificial ageing. The irregular trend is more pronounced in the natural ageing of coated samples than in those without hydrophobic treatments, which can be attributed to the degradation of the coatings. In contrast, in QUV-spray accelerated weathering,  $\Delta E\%$  regularly increased, as shown by the samples without any treatment. Furthermore,  $\Delta E\%$  values measured during artificial degradation were lower than those obtained in natural ageing, confirming that natural ageing is more severe.



**Figure 7.** Colour variation and colour difference,  $\Delta E\%$ . An overall whitening of all stones can be seen.  $\Delta E\%$  of stones before, during, and after natural and QUV-spray ageing. Irregular trends characterised almost all samples during natural ageing. In the QUV-chamber,  $\Delta E\%$  increased regularly, probably due to the limited and fixed parameters of the ASTM G154-cycle7.

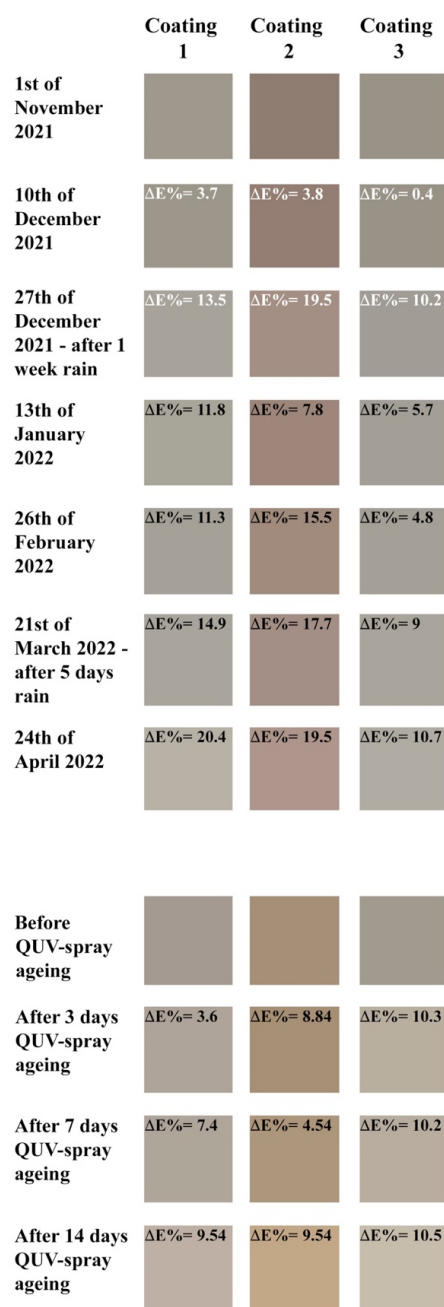


**Figure 8.** Colour variation and colour distance ( $\Delta E\%$ ) of blue limestone coated with hydrophobic coating 1 (aminopropyltriethoxysilane), coating 2 (aminopropyltriethoxysilane in 1:2 dilution), and coating 3 (tripotassium propylsilanetriolate). An overall whitening of all stones was discerned.  $\Delta E\%$  of stones before, during, and after natural and QUV-spray ageing. An irregular trend characterised almost all samples during natural ageing. In the chamber,  $\Delta E\%$  increased regularly, probably due to the limited and fixed parameters of the ASTM G154-cycle7.

Additionally, surface texture can influence the retention of moisture, which can impact the weathering process. Polished surfaces are more resistant to weathering compared to a rough or porous surfaces, as they reduce the penetration of water. Accordingly, even the penetration depth of the hydrophobic coatings is significantly reduced, also influencing durability of the product itself.

### 5.3. Micro-Texture and Superficial Roughness: The Role of Water

Besides providing aesthetic value, polishing enhances stone's durability, reducing absorption of water in the liquid and vapour phases. Therefore, polishing is often chosen as a natural means of stone protection [24].

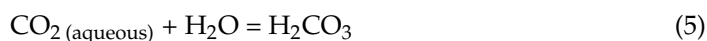
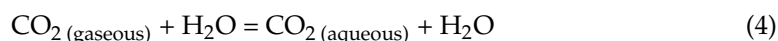
Changes in surface roughness can cause a loss of stone's glossy aspect and can cause discolouration [39], affecting the aesthetic and economic value imparted by polishing.

The microtexture images obtained through scanning electron microscopy (SEM) and the calculation of digital superficial roughness using parameters such as Ra, Rz, and Rq (as shown in Figures 9 and 10) provide compelling evidence of the significant changes induced in the superficial texture by natural and artificial weathering. The results clearly demonstrate that the weathering process leads to a general trend of increased roughness and irregularity in the surface texture, regardless of whether the samples are limestones or marbles. These changes in superficial texture were observed after both natural and artificial weathering, and a comprehensive analysis of microtexture and superficial roughness was conducted before and after these weathering events. One of the most representative parameters for comparing the changes in texture before and after weathering is Ra, which generally shows higher values after natural weathering, except in the cases of Rosa and Lioz A. For instance, in Rosa, Ra increased from 0.183  $\mu\text{m}$  before ageing to 0.482  $\mu\text{m}$  after natural ageing, and further to 1.008  $\mu\text{m}$  after QUV-spray ageing. Similarly, in Lioz A, Ra showed a similar trend, with values of 0.082  $\mu\text{m}$  before ageing, 1.175  $\mu\text{m}$  after natural ageing, and 1.436  $\mu\text{m}$  after QUV-spray ageing. In the case of blue limestone, Ra remained consistently high at 0.981  $\mu\text{m}$  after 6 months of natural ageing, and reached 0.914  $\mu\text{m}$  after QUV-spray ageing, indicating that this stone is highly susceptible to rapid alteration under any weathering conditions.

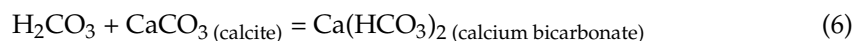
These findings support the hypothesis that weathering significantly affects superficial texture, resulting in increased roughness and irregularity in both limestones and marbles, as shown by the changes in Ra values before and after natural and artificial ageing.

The rugosity of blue limestone treated with hydrophobic coatings (Figure 10) underlines the degradation susceptibility of the coatings during natural exposure to slightly acidic rainwater and, in the QUV-spray chamber, to the other measured parameters.

The general theory underlying the process of carbonate rock-alteration and its implications for stone material-alteration have already been discussed [24,40], and deal with the dissolution capacity of water, which is correlated with the temperature, TDS, and salinity. The solubility constant,  $K_{01}$ , of  $\text{CO}_2$  is equal to  $3.95 \times 10^{12}$  at 20 °C for natural water with a TDS of 0, while sea water has a TDS of 40 g/L and a  $K_{01}$  of  $\text{CO}_2$  of  $3.2 \times 10^{12}$ . This means that low salinity water and distillate water, such as rainwater and the QUV-spray collected, promote the dissolution of gaseous  $\text{CO}_2$  in water, increasing the concentration of  $\text{H}_2\text{CO}_3$  in aqueous solution. The chemical reactions are as follows:



$\text{H}_2\text{CO}_3$  has a strong dissolution capability against carbonate stone, especially from the early reaction stages until equilibrium is reached (buffering effect), as illustrated by the following congruent chemical reaction:



At 25 °C, calcite has a solubility of 0.014 g/L and calcium bicarbonate has a solubility of 166 g/L, meaning the latter is easily leached by runoff and the rain.

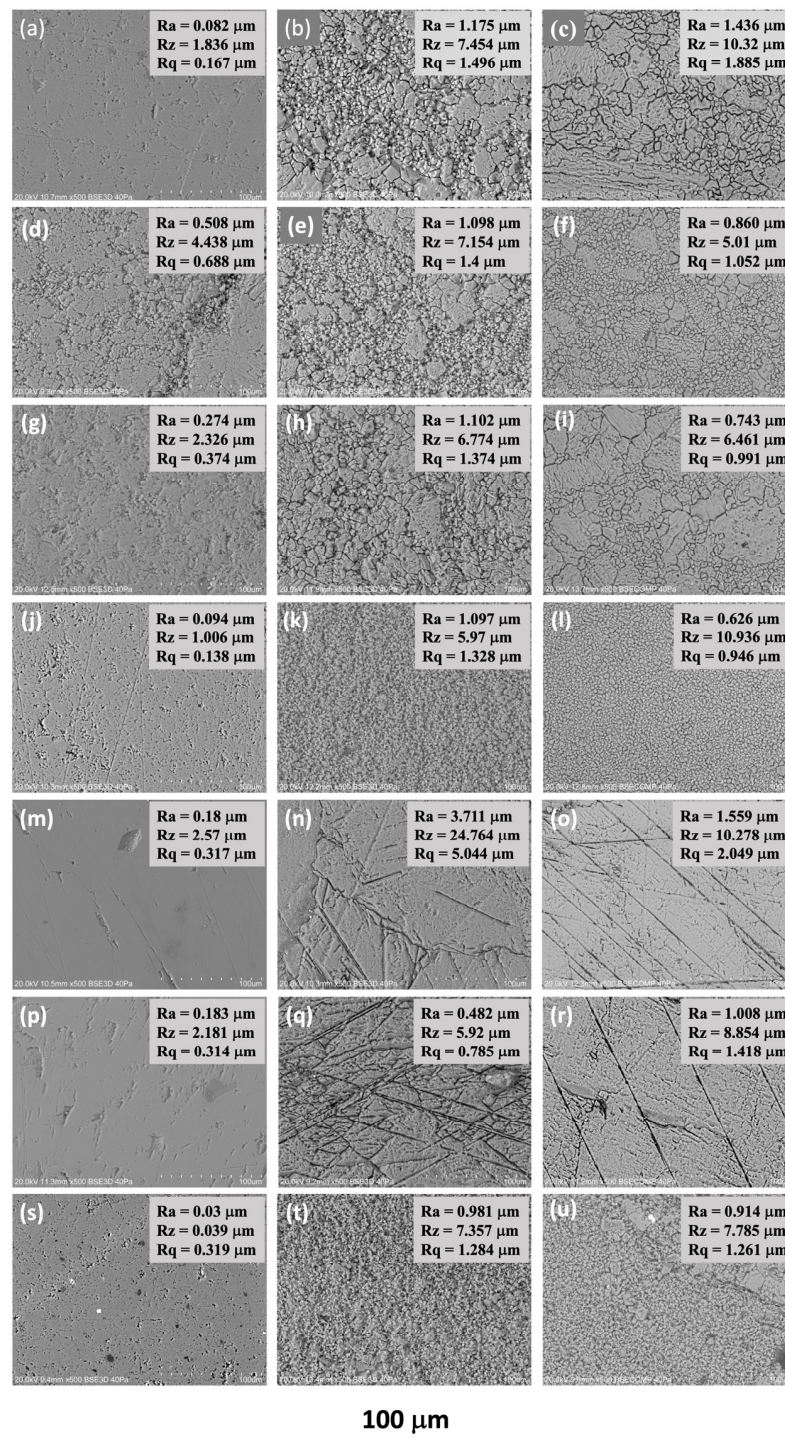


**Figure 9.** Micro-texture analyses through SEM and according to the roughness parameters, Ra, Rz, and Rq, measured with the digital rugosimeter. (a–c) Lioz A before and after natural ageing and after QUV-spray ageing, (d–f) Lioz B before and after natural ageing and after QUV-spray ageing, (g–i) Lioz C before and after natural ageing and after QUV-spray ageing, (j–l) Alpinina before and after natural ageing and after QUV ageing, (m–o) BW marble before and after natural ageing and after QUV ageing, (p–r) Rosa before and after natural ageing and after QUV ageing, (s–u) Blue limestone before and after natural ageing and after QUV ageing. The data support the argument that weathering significantly affects superficial texture, resulting in increased roughness and irregularity in both limestones and marbles, as evidenced by the changes in Ra values before and after natural and artificial weathering.

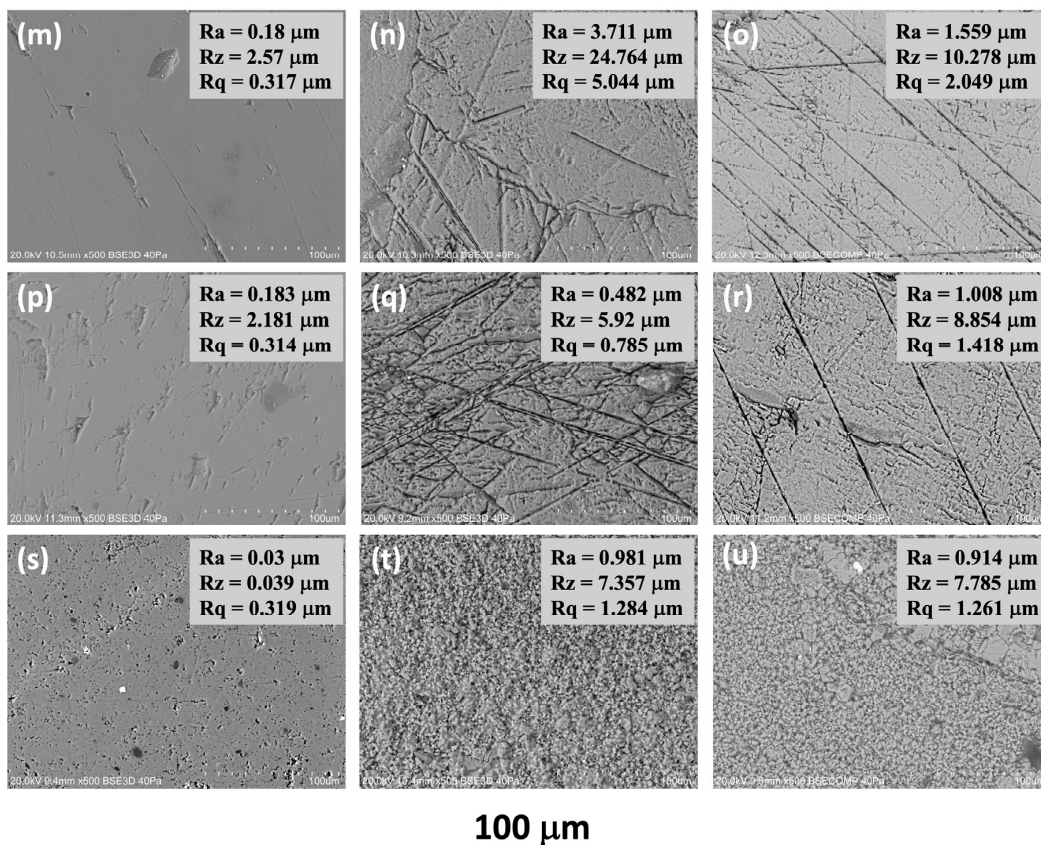


**Figure 10.** Micro-texture of blue limestone coated with hydrophobics. (m) coating 1 before the tests, (n) after natural ageing, and (o) after QUV-spray ageing; (p) coating 2 before the tests, (q) after natural ageing, and (r) after QUV-spray ageing; (s) coating 3 before the test, (t) after natural ageing, and (u) after QUV-spray ageing. The white minerals and spots are pyrite inclusions.

Indeed, the textural analyses and data of rugosity confirm that changes in surface roughness due to water-carbonate interactions cause the loss of the stone's glossy aspect and discolouration, affecting the aesthetic and the economic value imparted by polishing. This shows that polished stones are more suitable as decorative elements in indoor environments, where they are protected from weathering agents, while rougher surfaces (hammered, brushed, flame-treated, etc.) are proper for outdoor environments, where safety and footfall-resistance requirements must be guaranteed.

#### 5.4. Wetting, Contact Angle, and Permeability

Wettability is a property that expresses the spreading out of a liquid when it is in contact with a solid surface. It is measured by the contact angle [41], which is the angle formed between the solid/liquid interface and the liquid/vapour interface when the three phases (solid, liquid, vapour) are in equilibrium, defined as the equilibrium Young contact angle [42]. The wettability relates to the cohesive forces of the liquid molecules and to the adhesive forces (electrostatic force due to hydrogen bonds) between the liquid and the solid surface, upon which the superficial tension of the liquid and the surface free energy of the solid surface depend [43]. Young's model only considers intermolecular interaction and, the stronger the cohesive forces are with respect to the adhesion forces, the lower the wettability. Afterwards, Wenzel introduced the contributions of surface regularity/micro-roughness to wettability [44]. Furthermore, Cassie and Baxter developed a model that also considers how the air trapped between the drops and the asperities of porous materials could increase the degree of hydrophobicity [45,46].

The application of protective coatings (mainly organic) aims to reduce the electrostatic attraction between the polar molecules of water and the electronegative groups of stone materials (i.e., carbonates, silicates, oxides, aluminates, etc.) trying to reproduce the so-called “lotus-leaf effect” or the “rose petal effect” [47].

The static contact angle was measured to calculate the degree of hydrophobicity of blue limestone because it is the most susceptible to pathologies. Images of the contact angle in uncoated stones and those coated with coating 1 (aminopropyltriethoxysilane), coating 2 (aminopropyltriethoxysilane in 1:2 and dilution), and coating 3 (tripotassium propylsilanetriolate) are presented in Figure 11.

Untreated blue limestone samples present a 61° contact angle. This value is relatively high because the polished finishing turns the surface smooth, and the low micro-roughness reduces the adhesion forces within the water/stone matrix. Coatings 1, 2, and 3 have pre-ageing contact angles of 103°, 95°, and 106°, respectively.

Both natural and artificial weathering reduce the contact angle value. Lower values (from 35° to 38°) appeared in samples subjected to UVA radiation and spray and moisture accelerated ageing. Natural ageing affected the decrease in the contact angles of coating 1 and coating 3 (68–60°) less, while the reasonable value of 45° after natural ageing for coating 2 is attributable to the dilution of coating 1.

In natural ageing, the loss of hydrophobicity confirms that rainwater with slight acidity and a low TDS content is capable of dissolving the stone matrix and damaging the protective coatings. During winter, it is plausible that the solar radiation had a marginal contribution to the depolymerisation of the coating.

Solar radiation, mostly UV spectra, exacerbates photochemical instabilities and causes polymer scission/crosslinking of molecules (“photodegradation”), while high temperatures and moisture can produce thermal degradation and hydrolysis, accelerating the photodegradation process [48,49].

During natural ageing, solar radiation ranges from a daily average of 81 W/m<sup>2</sup> in December to a daily average of 240 W/m<sup>2</sup> in April, in contrast to the solar irradiation ageing occurring in summer months, which has a daily average of 326 W/m<sup>2</sup>. Coated samples aged with QUV-spray also suffer the depolymerisation of organic chains (both of organic matter naturally present in the stone and organic coatings) induced by continued UVA at 1.55 W/m<sup>2</sup> (for a total of 112 h). However, any significant expected yellowing of the surfaces imputable to UV decay [50,51] was not detected after fourteen days of ageing because the coatings were completely leached out.

UV radiation interacts with organic coatings, forming free radicals that react with oxygen present in the atmosphere, degrading organic structures. Free radicals replace the carbonyl groups (or other chromophore groups) of polymers and alter molecular weight distributions [52], resulting in a loss of hydrophobicity [53].

Furthermore, in the QUV-spray chamber, UV decay is also associated with thermal shock and hydrolysis [49], as declared by the equipment manufacturer; after the UVA cycle at 60 °C, the spray cycle runs with distilled water (pH = 6.45) at 20 °C for 15 min, resulting in a thermal shock impact.

Water vapour permeability regulates moisture diffusion through porous media and vapour diffusion affects the drying rate of stones. The water vapour transmission should be natural to prevent the formation of a “vapour barrier”, which can lead to interstitial condensation that triggers degradation phenomena in the stone’s inner matrix [54,55]. If the vapour permeability or the water vapour flux before and after any ageing and treatment are similar, the stones are resistant to thermo-hygrometric variations [56].

In Table 3, the water vapour flux (Gw) and water vapour permeability (Wvp) are reported along with their respective variations ( $\Delta\%$ ) after natural weathering and QUV-spray ageing. The observations reveal a consistent decrease in both water vapour flux and water vapour permeability compared to the initial values, underscoring the damaging effects of ageing on the hygric properties of the samples.

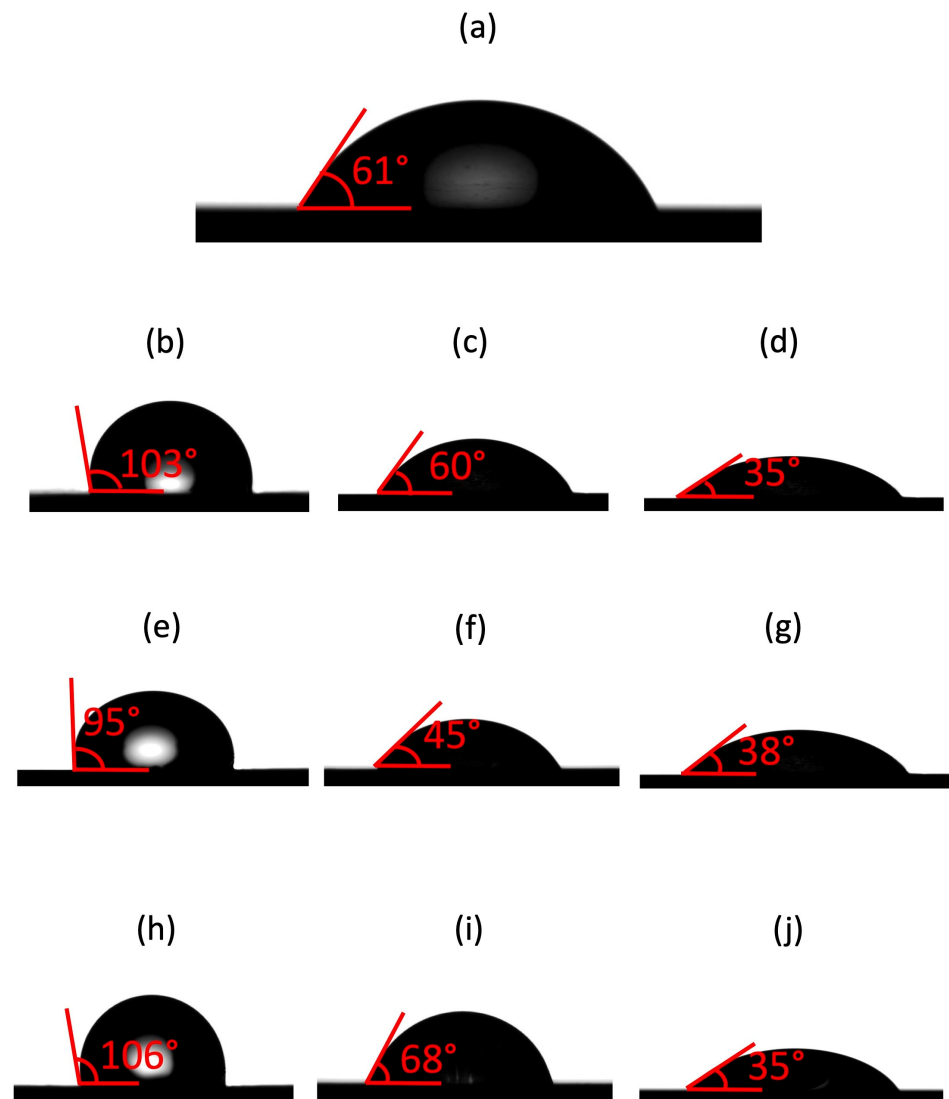


**Figure 11.** Contact angles of blue limestone. (a) Untreated blue limestone; (b–d) coating 1 before the tests, after natural ageing, and after QUV-spray ageing; (e–g) coating 2 before the tests, after natural ageing, and after QUV-spray ageing; (h–j) coating 3 before the test, after natural ageing, and after QUV-spray ageing, respectively.

Notably, the most severe decay in hygric properties was observed after six months of natural ageing, except for Alpinina limestone and BW marble, which showed relatively better performance. In contrast, Rosa showed similar  $\Delta\%$  values after both natural and artificial weathering, indicating its vulnerability to ageing.

Interestingly, samples treated with hydrophobics showed minimal changes in water vapour diffusion and permeability, closely resembling the initial values. This can be attributed to the protective coatings' inhibitory effects on stone alteration during the early stages of ageing, as evidenced by the sustained glossiness even after three days and seven days of ageing.

Overall, it can be concluded that prolonged exposure to low pH and low TDS water, and its resulting interaction with the stone matrix, is the primary cause of degradation in stone texture, finishing, and, therefore, the protective coatings. Furthermore, during accelerated ageing, the high UVA irradiance of the QUV-spray chamber and the associated high temperature and moisture aggravated the decay. These outcomes emphasise the need for effective protective measures to mitigate such degradation of polished building stones used in outdoor environments.

**Table 3.** Water vapour flux,  $G_w$ , and water vapour permeability,  $W_{VP}$ , are reported with their respective variation,  $\Delta\%$ , after natural and QUV-spray ageing.

	Before Test		After Natural Ageing				After QUV—Spray Ageing			
	$G_w$ (g/h)	$W_{VP}$ (g/m.s.Pa)	$G_w$ (g/h)	$W_{VP}$ (g/m.s.Pa)	$\Delta G_w$ (%)	$\Delta W_{VP}$ (%)	$G_w$ (g/h)	$W_{VP}$ (g/m.s.Pa)	$\Delta G_w$ (%)	$\Delta W_{VP}$ (%)
Lioz A	$4.40 \times 10^{-3}$	$5.10 \times 10^{-12}$	$2.69 \times 10^{-3}$	$2.79 \times 10^{-12}$	−39%	−45%	$3.20 \times 10^{-3}$	$3.70 \times 10^{-12}$	−27%	−27%
Lioz B	$6.20 \times 10^{-3}$	$7.30 \times 10^{-12}$	$2.93 \times 10^{-3}$	$2.83 \times 10^{-12}$	−53%	−61%	$4.60 \times 10^{-3}$	$4.80 \times 10^{-12}$	−26%	−34%
Lioz C	$4.80 \times 10^{-3}$	$5.00 \times 10^{-12}$	$2.28 \times 10^{-3}$	$2.87 \times 10^{-12}$	−53%	−43%	$2.90 \times 10^{-3}$	$3.50 \times 10^{-12}$	−40%	−30%
Alpinina	$5.70 \times 10^{-3}$	$7.10 \times 10^{-12}$	$2.75 \times 10^{-3}$	$3.47 \times 10^{-12}$	−52%	−51%	$2.19 \times 10^{-3}$	$2.27 \times 10^{-12}$	−62%	−68%
BW marble	$6.50 \times 10^{-3}$	$8.10 \times 10^{-12}$	$4.15 \times 10^{-3}$	$5.16 \times 10^{-12}$	−36%	−36%	$3.30 \times 10^{-3}$	$4.10 \times 10^{-12}$	−49%	−49%
Rosa marble	$5.40 \times 10^{-3}$	$6.50 \times 10^{-12}$	$4.92 \times 10^{-3}$	$5.97 \times 10^{-12}$	−9%	−8%	$4.80 \times 10^{-3}$	$6.00 \times 10^{-12}$	−11%	−8%
Blue limestone	$1.00 \times 10^{-02}$	$1.00 \times 10^{-11}$	$5.72 \times 10^{-3}$	$5.51 \times 10^{-12}$	−43%	−45%	$8.50 \times 10^{-3}$	$8.10 \times 10^{-12}$	−15%	−19%
Coating 1	$5.44 \times 10^{-3}$	$8.66 \times 10^{-12}$	$4.01 \times 10^{-3}$	$6.22 \times 10^{-12}$	−26%	−28%	$5.02 \times 10^{-3}$	$7.83 \times 10^{-12}$	−8%	−10%
Coating 2	$6.06 \times 10^{-3}$	$9.73 \times 10^{-12}$	$2.93 \times 10^{-3}$	$4.55 \times 10^{-12}$	−52%	−53%	$5.82 \times 10^{-3}$	$9.35 \times 10^{-12}$	−4%	−4%
Coating 3	$6.68 \times 10^{-3}$	$1.01 \times 10^{-11}$	$3.36 \times 10^{-3}$	$5.21 \times 10^{-12}$	−50%	−48%	$6.24 \times 10^{-3}$	$1.00 \times 10^{-11}$	−7%	<1%

## 6. Conclusions

The analytical approach proposed in this study intended to predict the behaviour of stones over time and to quantify the weathering effects due to natural and artificial ageing, complying with the demand of the natural stone stakeholders to increase awareness of the quality and value of natural stone building materials.

A comparison between six months of natural ageing (November 2021–April 2022) and artificial weathering with UVA radiation, moisture, and spray-accelerated weathering in a QUV-spray chamber (ASTM G154 cycle 7) was attempted for natural stone materials in a non-polluted environment (Évora, Portugal). For this purpose, mainly aesthetic features (gloss and colour) were monitored by cross-checking the different data during the natural weathering and after three, seven, and fourteen days of artificial weathering. Colour distance was mostly due to the discolouration of the surfaces (lightening) caused by the dulling of the glossy finishing when the stone surface became rougher, as ascertained through SEM-image interpretation and rugosity measurements. It was difficult to find a reliable temporal correlation between the two types of weathering based only on colour modifications, but the gloss measurement enabled important outcomes: (i) the high dissolving capacity of rainwater and the QUV-spray chamber distillate water maximises the opacification of the glossy surface; (ii) increases in roughness are the major cause of chromatic alteration and the loss of the aesthetic value of the stones, and they are linked to surface dissolution; (iii) measurement of gloss during natural and artificial weathering indicated that three days in the QUV-spray chamber correspond to five months of natural ageing. In blue limestone, this correlation corresponds to two months because of the presence of pyrite and organic matter, which are prone to faster alteration. In BW marble, three days of QUV-spray ageing correspond to six months of natural ageing, but the gloss was preserved to the end of the tests, showing the effect of the calcite grain size. It is important to highlight that the correlation between natural and artificial weathering is variable and strictly depends on the number of rainy days in outdoor environments.

Blue limestone treated with hydrophobics unexpectedly also suffered from pathologies, and after only one week of rain the gloss had been drastically reduced. Coating 1 (aminopropyltriethoxysilane) performed better for blue limestone protection up to three months. However, the stone surface completely lost its gloss after four months. Coating 2 (aminopropyltriethoxysilane in 1:2 dilution) and coating 3 (tripotassium propylsilanetriolate) presented premature inefficiency and lost the gloss after two months.

Measurement of the contact angle confirmed the short efficiency of the coatings after natural and artificial ageing. QUV-spray ageing had a stronger effect on the coatings and the superficial texture degradation compared to natural ageing. The artificial ageing enhanced the depolymerisation induced by  $1.55 \text{ W/m}^2$  UVA radiation at  $60 \text{ }^\circ\text{C}$ . This effect was also intensified by the cycle water spray at  $20 \text{ }^\circ\text{C}$ , which led to thermal shock in the samples. These findings indicate that even if a product is proficient, it may not be suitable for use on all types of surfaces. In this case, the product's application on a low porosity stone with a polished finish led to a loss of efficiency and deterioration. The water vapour permeability and water vapour flux values decreased compared with the initial values in both natural and artificial weathering. Greater declines in the stones' hygric properties were detected in natural ageing in all samples except for Alpinina limestone and BW marble.

This study can open a new line of research on calcitic-based stone durability by developing comparative studies between natural and artificial weathering for a more accurate assessments of the long-term performance of natural stones in different climatic contexts.

To avoid threats, the first solution is prevention. This entails considering all direct or indirect actions aimed at preventing the occurrence or propagation of undesired alterations and pathologies, including those of an aesthetic nature. Even during the design phase, the sustainable selection of the most appropriate finish for the specific lithology and the surrounding environment can be regarded as a solution to the potential problems. It is crucial to always bear in mind that aesthetic considerations must not compromise the technical requirements of architectural quality, performance, durability, and safety.

**Supplementary Materials:** The following supporting information can be downloaded at: <https://www.mdpi.com/article/10.3390/heritage6060244/s1>, Annex S1: Evora climatic parameters from November 2021 to April 2022: (a) amount and relative humidity; (b) minimum, maximum and average temperature and (c) solar radiation expressed. All parameters are expressed as daily average; Annex S2: Air Quality Index map (a) and desert dust load in West-Central South Europe (b), after the database of [www.ventusky.com](http://www.ventusky.com) (accessed on 16 March 2022). Evora (Portugal) is blue marked. (a) Air Quality Index (AQI) depiction for Evora. The AQI scale ranges from 0 to 400, with higher values indicating poorer air quality. In this figure, the colour-coded legend represents different AQI categories: green (0–50) for good, yellow (51–100) for moderate, orange (101–150) for unhealthy for sensitive groups, red (151–200) for unhealthy, purple (201–300) for very unhealthy, and maroon (301–500) for hazardous. (b) The figure displays the dust load, expressed in  $\text{mg}/\text{m}^3$ , in various of North Africa and Portugal on 16 March. In Evora the load reached the  $600 \text{ mg}/\text{m}^3$ .

**Author Contributions:** C.L.: project administration, funding acquisition, conceptualisation, methodology, data curation, formal analysis, investigation, resources, software, validation, visualisation, writing—original draft, writing—review, and editing. F.S.: validation, visualisation, review, and editing. V.P.: visualisation, validation, review, and editing. M.A.: resources and validation. J.M.: supervision, funding acquisition, validation, visualisation, review, and editing. All authors have read and agreed to the published version of the manuscript.

**Funding:** Carla Lisci gratefully acknowledges FCT for the grant SFRH/BD/149699/2019 co-funded by the European Social Fund (ESF) and MEC national funds. Carla Lisci gratefully acknowledges Roberto Madorno for the constant technical-scientific support in the chemistry and the application of the protective treatments. Fabio Sitzia gratefully acknowledges the Recursos Humanos Altamente Qualificados for the contract with Ref. ALT2059-2019-24. Vera Pires gratefully acknowledges the Contrato Programa entre FCT e a Universidade de Évora no âmbito do concurso estímulo ao emprego científico institucional 2018. The authors gratefully acknowledge the following funding sources: INOVSTONE4.0 (POCI-01-0247-FEDER-024535), co-financed by the European Union through the European Regional Development Fund (FEDER) and Fundação para a Ciência e Tecnologia (FCT) under the project UID/Multi/04449/2013 (POCI-01-0145-FEDER-007649), and Fundacao para a Ciencia e Tecnologia (FCT) under the project UIDB/04449/2020 and UIDP/04449/2020. The authors gratefully acknowledge the European Communion—Portugal, Grant Contract number: Sustainable Stone by Portugal, Call: 2021-C05i0101-02—agendas/alianças mobilizadoras para a reindustrialização—PRR, Proposal: C632482988-00467016.

**Institutional Review Board Statement:** Not applicable.

**Informed Consent Statement:** Not applicable.

**Data Availability Statement:** Not applicable.

**Conflicts of Interest:** The authors declare no conflict of interest.

## References

1. Jelle, B.P. Accelerated climate ageing of building materials, components and structures in the laboratory. *J. Mater. Sci.* **2012**, *47*, 6475–6496. [[CrossRef](#)]
2. Sitzia, F.; Lisci, C.; Mirão, J. Building pathology and environment: Weathering and decay of stone construction materials subjected to a Csa mediterranean climate laboratory simulation. *Constr. Build. Mater.* **2021**, *300*, 124311. [[CrossRef](#)]
3. *EN-12371:2010*; Natural Stone Test Methods—Determination of Frost Resistance. Ente Nazionale Italiano di Unificazione: Roma, Italy, 2010.
4. *EN-14066:2011*; Natural Stone Test Methods—Determination of Resistance to Ageing by Thermal Shock. Ente Nazionale Italiano di Unificazione: Roma, Italy, 2011.
5. *EN 12370:2019*; Natural Stone Test Methods—Determination of Resistance to Salt Crystallisation. CEN-European Committee for Standardisation: Brussels, Belgium, 2019.
6. *EN 14147:2003*; Natural Stone Test Methods—Determination of Resistance to Ageing by Salt Mist. Ente Nazionale Italiano di Unificazione: Roma, Italy, 2003.
7. *EN 13919:2004 (retired)*; Natural Stone Test Methods—Determination of Resistance to Ageing by  $\text{SO}_2$  Action in the Presence of Humidity. Ente Nazionale Italiano di Unificazione: Roma, Italy, retired.
8. *BS EN ISO 11507:2007*; Paints and Varnishes—Exposure of Coatings to Artificial Weathering—Exposure to Fluorescent UV and Water. International Organization for Standardization (ISO): Geneva, Switzerland, 2007; pp. 1–17.

9. Sitzia, F.; Lisci, C.; Pires, V.; Alves, T. Laboratorial Simulation for Assessing the Performance of Slates as Construction Materials in Cold Climates. *Appl. Sci.* **2023**, *13*, 2761. [[CrossRef](#)]
10. *EN ISO 16474:2021*; Paints and Varnishes—Methods of Exposure to Laboratory Light Sources. International Organization for Standardization (ISO): Geneva, Switzerland, 2021.
11. *ISO 11507:2007*; Exposure of Coatings to Artificial Weathering—Exposure to Fluorescent UV and Water. International Organization for Standardization (ISO): Geneva, Switzerland, 2007.
12. *ASTM G154 C.7:2006*; Resistance of a Nonmetallic Material to Simulated Sunlight and Moisture Exposure. ASTM International: West Conshohocken, PA, USA, 2006.
13. *EOTA TR 010*; Exposure Procedure for Artificial Weathering. European Organisation for Technical Assessment: Brussels, Belgium, 2004.
14. *EN 17036:2018*; Conservation of Cultural Heritage. Artificial Ageing by Simulated Solar Radiation of the Surface of Untreated or Treated Porous Inorganic Materials. Ente Nazionale Italiano di Unificazione: Roma, Italy, 2018.
15. Tokarský, J.; Ščučka, J.; Martinec, P.; Mamulová Kutláková, K.; Peikertová, P.; Lipina, P. Long-term effect of weather in Dfb climate subtype on properties of hydrophobic coatings on sandstone. *J. Build. Eng.* **2022**, *52*, 104383. [[CrossRef](#)]
16. Orłowsky, J.; Braun, F.; Groh, M. The influence of 30 years outdoor weathering on the durability of hydrophobic agents applied on obernkirchener sandstones. *Buildings* **2020**, *10*, 18. [[CrossRef](#)]
17. García, O.; Malaga, K. Definition of the procedure to determine the suitability and durability of an anti-graffiti product for application on cultural heritage porous materials. *J. Cult. Herit.* **2012**, *13*, 77–82. [[CrossRef](#)]
18. Bellopede, R.; Castelletto, E.; Marini, P. Ten years of natural ageing of calcareous stones. *Eng. Geol.* **2016**, *211*, 19–26. [[CrossRef](#)]
19. Bracci, S.; Melo, M.J. Correlating natural ageing and Xenon irradiation of Paraloid® B72 applied on stone. *Polym. Degrad. Stab.* **2003**, *80*, 533–541. [[CrossRef](#)]
20. Striani, R.; Corcione, C.E.; Anna, G.D.; Frigione, M. Progress in Organic Coatings Durability of a sunlight-curable organic—Inorganic hybrid protective coating for porous stones in natural and artificial weathering conditions. *Prog. Org. Coat.* **2016**, *101*, 1–14. [[CrossRef](#)]
21. Sitzia, F.; Lisci, C.; Mirão, J. Accelerate ageing on building stone materials by simulating daily, seasonal thermo-hygrometric conditions and solar radiation of Csa Mediterranean climate. *Constr. Build. Mater.* **2021**, *266*, 121009. [[CrossRef](#)]
22. Lisci, C.; Sitzia, F.; Pires, V.; Mirao, J. The effects of QUV- spray accelerate weathering tester on building stones durability. *J. Build. Pathol. Rehabil.* **2022**, *7*, 60. [[CrossRef](#)]
23. Urosevic, M.; Sebastián, E.; Cardell, C. An experimental study on the influence of surface finishing on the weathering of a building low-porous limestone in coastal environments. *Eng. Geol.* **2013**, *154*, 131–141. [[CrossRef](#)]
24. Sitzia, F.; Lisci, C.; Mirão, J. The interaction between rainwater and polished building stones for flooring and cladding—Implications in architecture. *J. Build. Eng.* **2022**, *52*, 104495. [[CrossRef](#)]
25. Columbu, S.; Palomba, M.; Sitzia, F.; Carcangiu, G.; Meloni, P. Pyroclastic Stones as Building Materials in Medieval Romanesque Architecture of Sardinia (Italy): Chemical-Physical Features of Rocks and Associated Alterations. *Int. J. Archit. Herit.* **2022**, *16*, 49–66. [[CrossRef](#)]
26. Sharma, G. *Digital Color Imaging Handbook*; CRC Press: Boca Raton, FL, USA, 2017; ISBN 9781420041484.
27. *EN 15886:2010*; Conservation of Cultural Property—Test Methods—Colour Measurement of Surfaces. Ente Nazionale Italiano di Unificazione: Roma, Italy, 2010.
28. *EN Standard 15803*; Conservation of Cultural Property—Test Methods—Determination of Water Vapour Permeability ( $\delta p$ ). CEN: Brussels, Belgium, 2019.
29. *EN 15802:2010*; Conservation of Cultural Property—Test Methods—Determination of Static Contact Angle. Ente Nazionale Italiano di Unificazione: Roma, Italy, 2010.
30. Goudie, A.S.; Middleton, N.J. Saharan dust storms: Nature and consequences. *Earth-Sci. Rev.* **2001**, *56*, 179–204. [[CrossRef](#)]
31. Zhang, D.D.; Peart, M.R.; Jim, C.Y.; La, J. Alkaline rains on the Tibetan Plateau and their implication for the original pH of natural rainfall. *J. Geophys. Res. Atmos.* **2002**, *107*, ACH 9-1–ACH 9-6. [[CrossRef](#)]
32. Folk, R.L. *Petrologie of Sedimentary Rocks*; Hemphill Publ. Company: Austin, TX, USA, 1974. [[CrossRef](#)]
33. Dias, L.; Rosado, T.; Coelho, A.; Barrulas, P.; Lopes, L.; Moita, P.; Candeias, A.; Mirão, J.; Teresa Caldeira, A. Natural limestone discolouration triggered by microbial activity—A contribution. *AIMS Microbiol.* **2018**, *4*, 594–607. [[CrossRef](#)] [[PubMed](#)]
34. Pires, V.; Amaral, P.M.; Simão, J.A.R.; Galhano, C. Experimental procedure for studying the degradation and alteration of limestone slabs applied on exterior cladding. *Environ. Earth Sci.* **2022**, *81*, 59. [[CrossRef](#)]
35. Tugrul, A.; Zarif, I.H. Engineering aspects of limestone weathering in Istanbul, Turkey. *Bull. Eng. Geol. Environ.* **2000**, *58*, 191–206. [[CrossRef](#)]
36. Sousa, L.; Menningen, J.; López-Doncel, R.; Siegesmund, S. Petrophysical properties of limestones: Influence on behaviour under different environmental conditions and applications. *Environ. Earth Sci.* **2021**, *80*, 814. [[CrossRef](#)]
37. Akram, M.S.; Farooq, S.; Naeem, M.; Ghazi, S. Prediction of mechanical behaviour from mineralogical composition of Sakesar limestone, Central Salt Range, Pakistan. *Bull. Eng. Geol. Environ.* **2017**, *76*, 601–615. [[CrossRef](#)]
38. Khanlari, G.; Abdilor, Y. Influence of wet–dry, freeze–thaw, and heat–cool cycles on the physical and mechanical properties of Upper Red sandstones in central Iran. *Bull. Eng. Geol. Environ.* **2015**, *74*, 1287–1300. [[CrossRef](#)]

39. Benavente, D.; Martínez-Verdú, F.; Bernabeu, A.; Viqueira, V.; Fort, R.; García del Cura, M.A.; Illueca, C.; Ordóñez, S. Influence of Surface Roughness on Color Changes in Building Stones. *Color Res. Appl.* **2003**, *28*, 343–351. [[CrossRef](#)]
40. Millero, F.J.; Roy, R.N. A Chemical Equilibrium Model for the Carbonate System in Natural Waters. *Croat. Chem. Acta* **1997**, *70*, 1–38.
41. Lettieri, M.; Masieri, M.; Frigione, M. Novel Nano-Filled Coatings for the Protection of Built Heritage Stone Surfaces. *Nanomaterials* **2021**, *11*, 301. [[CrossRef](#)] [[PubMed](#)]
42. Young, T. An essay on cohesion of fluids. *Philos. Trans. R. Soc. London* **1805**, *95*, 65–87.
43. Clegg, C. *Contact Angle Made Easy*; Clegg, C., Ed.; 2013; ISBN 9781300662983. Available online: [https://www.researchgate.net/publication/305279668\\_Contact\\_Angle\\_Made\\_Easy](https://www.researchgate.net/publication/305279668_Contact_Angle_Made_Easy) (accessed on 4 May 2023).
44. Wenzel, R.N. Resistance of solid surfaces to wetting by water. *Ind. Eng. Chem.* **1936**, *28*, 988–994. [[CrossRef](#)]
45. Cassie, A.B.D.; Baxter, S. Wettability of porous surfaces. *Trans. Faraday Soc.* **1944**, *40*, 546–551. [[CrossRef](#)]
46. Hansson, P.M.; Skedung, L.; Claesson, P.M.; Swerin, A.; Schoelkopf, J.; Gane, P.A.C.; Rutland, M.W.; Thormann, E. Robust hydrophobic surfaces displaying different surface roughness scales while maintaining the same wettability. *Langmuir* **2011**, *27*, 8153–8159. [[CrossRef](#)]
47. Parvate, S.; Dixit, P.; Chattopadhyay, S. Superhydrophobic Surfaces: Insights from Theory and Experiment. *J. Phys. Chem. B* **2020**, *124*, 1323–1360. [[CrossRef](#)]
48. Chiavari, C.; Balbo, A.; Bernardi, E.; Martini, C.; Zanotto, F.; Vassura, I.; Bignozzi, M.C.; Monticelli, C. Organosilane coatings applied on bronze: Influence of UV radiation and thermal cycles on the protectiveness. *Prog. Org. Coat.* **2015**, *124*, 1323–1360. [[CrossRef](#)]
49. Gupta, G.; Pathak, S.S.; Khanna, A.S. Anticorrosion performance of eco-friendly silane primer for coil coating applications. *Prog. Org. Coat.* **2012**, *74*, 106–114. [[CrossRef](#)]
50. Borsoi, G.; Esteves, C.; Flores-Colen, I.; Veiga, R. Effect of hygrothermal aging on hydrophobic treatments applied to building exterior claddings. *Coatings* **2020**, *10*, 363. [[CrossRef](#)]
51. De Vries, J.; Polder, R.B. Hydrophobic treatment of concrete. *Constr. Build. Mater.* **1997**, *11*, 259–265. [[CrossRef](#)]
52. Rabek, J.F. *Polymer Photodegradation. Mechanism and Experimental Methods*; Springer: Dordrecht, The Netherlands, 1995; ISBN 978-94-011-1274-1.
53. Ghasemi-Kahrizsangi, A.; Neshati, J.; Shariatpanahi, H.; Akbarinezhad, E. Improving the UV degradation resistance of epoxy coatings using modified carbon black nanoparticles. *Prog. Org. Coat.* **2015**, *85*, 199–207. [[CrossRef](#)]
54. BS 5250:2011 + A1:2016; Code of Practice for Control of Condensation in Buildings. British Standards Institution: Chiswick, UK, 2011.
55. Calia, A.; Lettieri, M.; Mecchi, A.; Quarta, G. The role of the petrophysical characteristics on the durability and conservation of some porous calcarenites from Southern Italy. *Geol. Soc. Spec. Publ.* **2016**, *416*, 183–201. [[CrossRef](#)]
56. Erba, S.; Daniotti, B.; Rosina, E.; Sansonetti, A.; Paolini, R. Evaluation of Moisture Transfer to Improve the Conservation of Tiles Finishing Facades. In *Recent Developments in Building Diagnosis Techniques*; Springer: Singapore, 2016.

**Disclaimer/Publisher’s Note:** The statements, opinions and data contained in all publications are solely those of the individual author(s) and contributor(s) and not of MDPI and/or the editor(s). MDPI and/or the editor(s) disclaim responsibility for any injury to people or property resulting from any ideas, methods, instructions or products referred to in the content.